

# Kidney preservation by bone marrow cell transplantation in hereditary nephropathy

Brian A. Yeagy<sup>1</sup>, Frank Harrison<sup>1</sup>, Marie-Claire Gubler<sup>2</sup>, James A. Koziol<sup>1</sup>, Daniel R. Salomon<sup>1</sup> and Stephanie Cherqui<sup>1</sup>

<sup>1</sup>Department of Molecular and Experimental Medicine, The Scripps Research Institute, La Jolla, California, USA and <sup>2</sup>Inserm 983, Universite Paris Descartes, Necker Enfants Malades Hospital, Paris, France

**The prospect of cell-based therapy for kidney disease remains controversial despite its immense promise. We had previously shown that transplanting bone marrow and hematopoietic stem cells could generate renal cells and lead to the preservation of kidney function in a mouse model for cystinosis (*Ctns*<sup>-/-</sup>) that develops chronic kidney injury, 4 months post transplantation. Here, we determined the long-term effects of bone marrow stem cell transplantation on the kidney disease of *Ctns*<sup>-/-</sup> mice 7 to 15 months post transplantation. Transfer of bone marrow stem cells expressing a functional *Ctns* gene provided long-term protection to the kidney. Effective therapy, however, depended on achieving a relatively high level of donor-derived blood cell engraftment of *Ctns*-expressing cells, which was directly linked to the quantity of these cells within the kidney. In contrast, kidney preservation was dependent neither on renal cystine content nor on the age of the mice at the time of transplant. Most of the bone marrow-derived cells within the kidney were interstitial and not epithelial, suggesting that the mechanism involved an indirect protection of the tubules. Thus, our model may help in developing strategies to enhance the potential success of cell-based therapy for kidney injury and in understanding some of the discrepancies currently existing in the field.**

*Kidney International* advance online publication, 19 January 2011; doi:10.1038/ki.2010.537

KEYWORDS: bone marrow stem cells; chronic kidney injury; cystinosis; donor-derived blood cell engraftment

Chronic kidney disease is the progressive loss of kidney function over time that can lead to end-stage renal failure and increased cardiovascular disease and mortality.<sup>1-3</sup> This is a major health challenge, and developing new therapies is an important objective. A number of publications have raised the prospect of doing cell-based therapy for kidney injury and failure. However, though promising, the therapeutic potential of stem cell transplantation for renal disorders is still controversial.<sup>4-6</sup>

Some authors demonstrated that unfractionated bone marrow cells (BMCs) and hematopoietic stem cells (HSCs) could generate tubular cells and improve renal function.<sup>7,8</sup> Following a systemic injection of human HSCs 24 h post injury in immunodeficient mice, Li *et al.*<sup>9</sup> showed selective recruitment and localization of bone marrow-derived cells to the kidney vasculature, resulting in the improvement of the structural and functional recovery as well as the increased survival. Kalluri and colleagues<sup>10,11</sup> showed that BMC transplantation led to the formation of bone marrow-derived podocytes and mesangial cells in a mouse model for the hereditary nephropathy of Alport's syndrome.

On the other hand, some authors deny the possibility that renal cells can be derived from transplanted BMCs. One study concluded that intrarenal stem cells but not bone marrow-derived cells are responsible for the regeneration of kidney tissue after ischemic injury. Thus, injection of BMCs does not make any significant contribution to functional or structural recovery.<sup>12</sup> Others showed that bone marrow-derived cells within the kidney after injury were mostly cells of lymphoid lineage.<sup>13,14</sup> Stokman *et al.*<sup>15</sup> showed that renal failure after ischemia is improved by HSC mobilization using cytokines. However, in this model, the cytokines also altered the underlying inflammatory processes triggered by kidney injury, and there was no evidence of involvement of the mobilized HSCs.<sup>15</sup> Similarly, they showed that renal fibrosis was not improved by HSCs mobilized by stem cell factor and granulocyte-colony stimulating factor treatment after acute renal injury in mice.<sup>16</sup>

Given these controversies, it is important to develop new models for studying strategies to enhance the potential of success of cell-based therapy for kidney injury and in particular for chronic kidney injury. The mouse model for cystinosis,

**Correspondence:** Stephanie Cherqui, Department of Molecular and Experimental Medicine, The Scripps Research Institute, 10550 North Torrey Pines Road, La Jolla, California 92037, USA. E-mail: scherqui@scripps.edu

Received 25 June 2010; revised 20 October 2010; accepted 16 November 2010

**Table 1 | Serum and urine analyses for renal function**

	Wild type (n=27)	<i>Ctns</i> <sup>-/-</sup> (n=29)	Treated <i>Ctns</i> <sup>-/-</sup> (n=30)	Treated <i>Ctns</i> <sup>-/-</sup> <50% engraftment (n=9)	Treated <i>Ctns</i> <sup>-/-</sup> >50% engraftment (n=21)
<b>Serum</b>					
Creatinine (mg/dl)	0.25 ± 0.08	0.44 ± 0.19 <sup>a</sup>	0.36 ± 0.15 <sup>a,b</sup>	0.47 ± 0.14 <sup>a,c</sup>	0.31 ± 0.12 <sup>a,b,d</sup>
Creatinine clearance (ml/min)	0.08 ± 0.05	0.06 ± 0.03 <sup>a</sup>	0.05 ± 0.05 <sup>a</sup>	0.03 ± 0.01 <sup>a,b</sup>	0.06 ± 0.06 <sup>a,d</sup>
Urea (mg/dl)	64.36 ± 28.91	103.62 ± 28.19 <sup>a</sup>	108.26 ± 27.92 <sup>a</sup>	130.38 ± 26.06 <sup>a,b,c</sup>	98.31 ± 22.95 <sup>a,d</sup>
Phosphate (mg/dl)	11.78 ± 3.51	12.79 ± 2.18	13.77 ± 3.31 <sup>a</sup>	14.90 ± 5.24 <sup>a,b</sup>	13.26 ± 1.91 <sup>a</sup>
Alkaline phosphatase (IU/l)	54.19 ± 25.51	126.92 ± 58.32 <sup>a</sup>	119.87 ± 64.05 <sup>a</sup>	145.62 ± 63.83 <sup>a</sup>	108.27 ± 62.24 <sup>a</sup>
<b>Urine</b>					
Phosphate (μmol per 24 h)	2.39 ± 1.59	6.73 ± 5.27 <sup>a</sup>	4.81 ± 4.04 <sup>a</sup>	7.34 ± 5.75 <sup>a</sup>	3.72 ± 2.52 <sup>a,b</sup>
Protein (mg per 24 h)	16.53 ± 15.93	13.84 ± 10.89	10.25 ± 6.80 <sup>a</sup>	7.86 ± 5.61 <sup>a</sup>	11.27 ± 7.12
Volume (ml)	0.61 ± 0.31	1.73 ± 0.92 <sup>a</sup>	1.23 ± 0.85 <sup>a,b</sup>	1.50 ± 0.94 <sup>a</sup>	1.10 ± 0.80 <sup>a,b</sup>

<sup>a</sup>*P* < 0.05 compared with wild-type mice.<sup>b</sup>*P* < 0.05 compared with *Ctns*<sup>-/-</sup> mice.<sup>c</sup>*P* < 0.05 compared with treated *Ctns*<sup>-/-</sup> mice.<sup>d</sup>*P* < 0.05 compared with treated <50% engraftment *Ctns*<sup>-/-</sup> mice.

*Ctns*<sup>-/-</sup> mice, is an excellent model for chronic kidney disease. C57BL/6 *Ctns*<sup>-/-</sup> mice develop renal dysfunction as soon as 6 months of age and chronic renal failure by the age of 15 months, and cystine crystals accumulate progressively within interstitial and proximal tubular cells.<sup>17,18</sup> We demonstrated that, in this context, BMC-derived cells can efficiently get engrafted in the kidney tissue compartment, lead to a significant decrease in cystine content, and prevent the progression of kidney dysfunctions.<sup>19</sup> Indeed, 4 months post transplantation, 13% of the total renal cells as determined by quantitative PCR (qPCR) were derived from the infused wild-type BMCs expressing functional *Ctns*. These BMC-derived cells were predominately non-lymphoid lineage interstitial cells, but were also co-localized with distal and proximal tubular, glomerular, and endothelial cells. Moreover, the treated mice exhibited normal serum urea and creatinine levels in contrast to *Ctns*<sup>-/-</sup> mice treated with *Ctns*<sup>-/-</sup> BMCs at 4 months post transplantation. Mesenchymal stem cell transplantation in this model produced only a short-term improvement in renal function, perhaps by a paracrine mechanism previously demonstrated by others,<sup>20-22</sup> as there was little evidence of mesenchymal stem cell engraftment in the kidney.

In the present study, we investigated the long-term effects of bone marrow-derived stem cell transplantation on the kidney disease of treated *Ctns*<sup>-/-</sup> mice up to 15–17 months of age. We demonstrated that stem cell transplantation could prevent chronic kidney disease in this model. However, effective therapy depends on achieving a relatively high level of *Ctns*-expressing cells in the bone marrow, which is directly linked to the number of *Ctns*-expressing cells found within the kidney. In contrast, kidney repair was not dependent on the age of the mice at the time of transplantation; thus, kidney injury can be improved in animals transplanted after 6 months of age.

## RESULTS

We analyzed 30 C57BL/6 *Ctns*<sup>-/-</sup> mice transplanted for over 7 months with either BMCs (23 mice) or HSCs (7 mice). Of them, 15 were transplanted between 2 and 6 months of age

and 15 between 6 and 10 months of age. Transplanted cells were isolated from green fluorescent protein (GFP)-transgenic mice. In all, 29 non-treated *Ctns*<sup>-/-</sup> mice and 27 wild-type mice were used as controls, with both groups age-matched with the treated mice. Mice were killed between 15 and 17 months of age for a complete analysis, including cystine levels, kidney *Ctns* expression, renal function, and histology. We determined the level of bone marrow engraftment of transplanted cells measured as the percentage of GFP<sup>+</sup> cells in the blood: levels ranged from 0.06 to 93.1%. The mean of donor-derived cells was 64 ± 29% and the mean contribution for each lineage was similar for BMCs and HSC-transplanted cells: 10 ± 5% T-lymphocytes, 21 ± 14% B-lymphocytes, and 14 ± 8% monocytes. The rest of GFP<sup>+</sup> cells were granulocytes.

### Renal function in treated *Ctns*<sup>-/-</sup> mice depends on blood engraftment but not on the age of transplantation

Serum creatinine levels were significantly lower in treated mice compared with *Ctns*<sup>-/-</sup> control mice, and the baseline polyuria of the treated *Ctns*<sup>-/-</sup> mice was improved (Table 1). However, renal function data showed an important variability in the treated mice; some mice exhibited normal kidney function and some had biochemical data similar to non-treated *Ctns*<sup>-/-</sup> mice. We demonstrated that the preservation of the kidneys in the treated mice was directly linked to a higher level of donor-derived BMC engraftment expressing a functional *Ctns* gene. Indeed, linear regression analyses of renal function data compared with that of blood engraftment demonstrated that serum creatinine and urea were significantly decreased as blood engraftment increased ( $F_{1,27} = 7.943$ ,  $P = 0.009$ ,  $R^2 = 0.227$  for creatinine, and  $F_{1,27} = 12.656$ ,  $P = 0.001$ ,  $R^2 = 0.319$  for urea; Figure 1a). In these regression analyses, initial tests for differences between BMC- and HSC-transplanted mice did not achieve statistical significance:  $F_{1,26} = 0.776$ ,  $P = 0.39$  for creatinine, and  $F_{1,26} = 1.286$ ,  $P = 0.27$  for urea). We also performed analyses of variance comparing age-matched wild-type mice, *Ctns*<sup>-/-</sup> control mice, and treated *Ctns*<sup>-/-</sup> mice, with blood engraftment

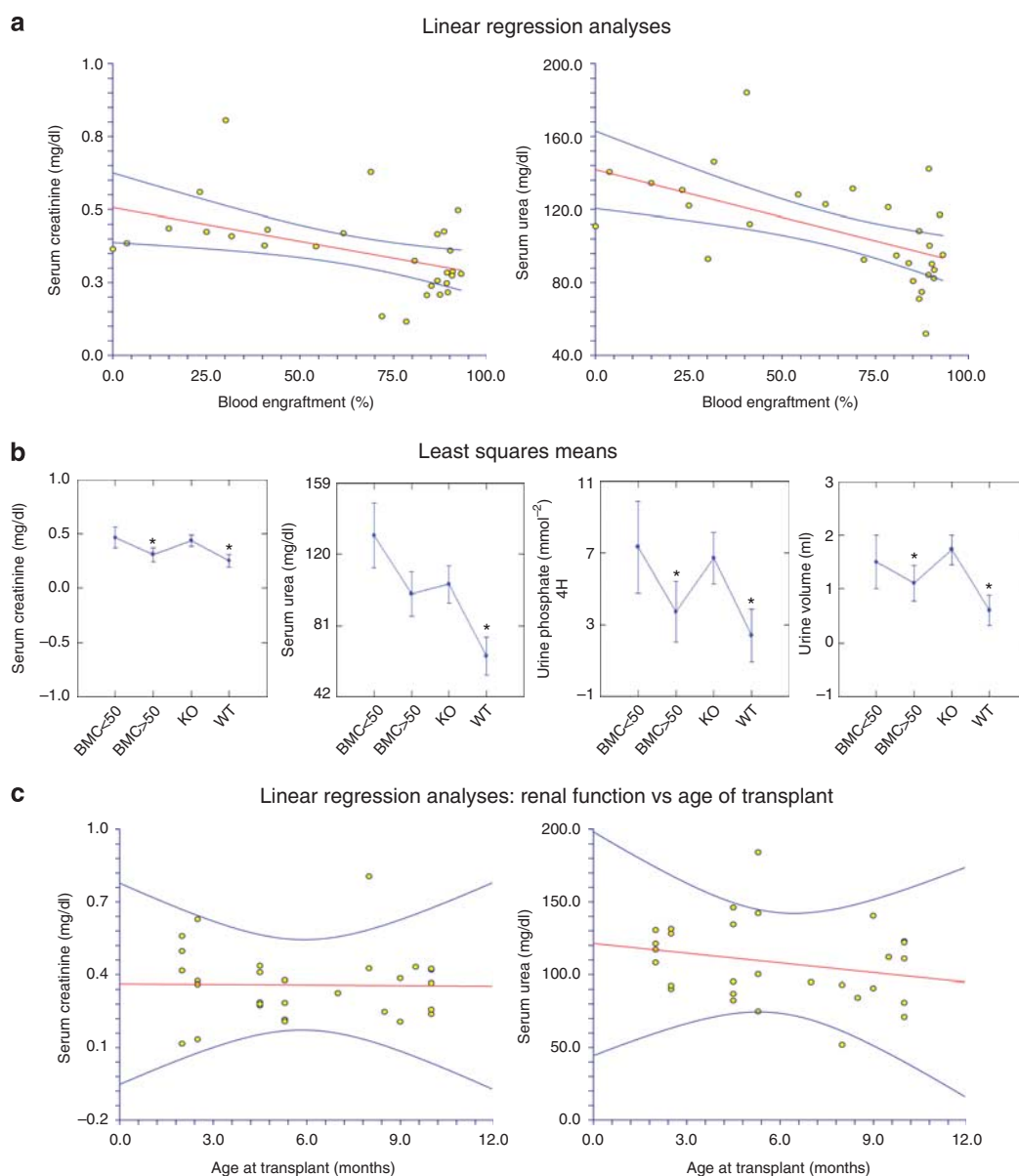


**Figure 1 | Statistical analyses of renal function data.** (a) Linear regression analyses of serum creatinine and urea compared with blood engraftment levels showing a decrease in creatinine and urea measures in mice with a high blood engraftment levels. The linear regression lines are depicted in red, and the corresponding 95% confidence bands about the lines are depicted in blue. (b) Least squares means and s.d. as determined from analyses of variance comparing wild-type mice, *Ctnt*<sup>-/-</sup> control mice, and treated *Ctnt*<sup>-/-</sup> mice with blood engraftment levels inferior and superior to 50% for serum creatinine, urine phosphate, and urine volume. Treated mice with blood engraftments superior to 50% had significantly improved serum creatinine, urine phosphate, and urine volume compared with *Ctnt*<sup>-/-</sup> mice and similar to wild-type mice. Serum urea is also improved in treated *Ctnt*<sup>-/-</sup> mice with a donor blood engraftment >50% compared with *Ctnt*<sup>-/-</sup> mice but the difference is not significant. (c) Linear regression analyses of serum creatinine and urea compared with age of transplantation showing no correlation between these parameters.

levels inferior and superior to 50% donor engraftment (Table 1). We found that treated mice with donor-derived cell engraftment inferior to 50% showed renal function data similar or worse than non-treated mice. In contrast, treated mice with engraftment superior to 50% had significantly improved serum creatinine, urine phosphate, and urine volumes compared with *Ctnt*<sup>-/-</sup> mice, achieving levels similar to the wild-type mice (Table 1 and Figure 1b). Serum urea is also improved compared with *Ctnt*<sup>-/-</sup> mice but the

difference is not significant (Table 1 and Figure 1b). Note that mice that underwent lethal irradiation and transplantation are less healthy overall in comparison with the wild-type and untreated cystinotic animals. This was confirmed by histological studies showing that transplanted wild-type mice also presented renal anomalies (see below). Thus, the fact that our measurements of kidney function in *Ctnt*<sup>-/-</sup> mice, which have more than 50% of their BMCs expressing a functional *Ctnt* gene, were consistently improved or

**Table 2 | Cystine content in multiple tissues of treated and control mice at 15–17 months old**

	Wild type	<i>Ctns</i> <sup>-/-</sup>	Treated <i>Ctns</i> <sup>-/-</sup>	Percentage decrease in cystine <sup>a</sup>
Brain	0.02+0.01 <sup>b</sup>	5.09+2.66	1.90+1.24 <sup>c</sup>	62.7
Eye	0.09+0.10	178.91+209.47	33.65+31.71 <sup>c</sup>	81.2
Heart	0.14+0.05	201.27+151.32	79.95+65.10 <sup>c</sup>	60.3
Kidney	0.19+0.05	519.42+564.42	239.09+227.70 <sup>c</sup>	54.0
Liver	0.02+0.01	151.13+55.01	5.23+3.70 <sup>c</sup>	96.5
Muscle	0.24+0.09	58.73+33.04	25.55+23.78 <sup>c</sup>	56.5
Spleen	0.06+0.03	379.06+193.40	27.30+30.98 <sup>c</sup>	92.8

<sup>a</sup>Percent decrease in cystine content in treated mice compared with *Ctns*<sup>-/-</sup> mice control.

<sup>b</sup>Cystine content is stated in nmol half-cystine per mg protein.

<sup>c</sup>*P*<0.05 compared with non-treated *Ctns*<sup>-/-</sup> mice.

even normalized clearly demonstrates the efficacy of this treatment.

On the other hand, based on analysis of variance, there is no significant difference in renal function between mice transplanted before and after 6 months of age (data not shown). This conclusion was confirmed by a linear regression analysis of renal function and age of transplant as continuous variables ( $F_{1,27} = 0.006$ ,  $P = 0.936$ ,  $R^2 = 0.001$  for creatinine, and  $F_{1,27} = 1.613$ ,  $P = 0.215$ ,  $R^2 = 0.056$  for urea; Figure 1c). In these regression analyses, initial tests for differences between BMC- and HSC-transplanted mice did not achieve statistical significance:  $F_{1,26} = 0.190$ ,  $P = 0.67$  for creatinine, and  $F_{1,26} = 0.078$ ,  $P = 0.78$  for urea).

#### Kidney *Ctns* expression but not kidney cystine content depends on blood engraftment in treated *Ctns*<sup>-/-</sup> mice

To determine the influence of donor-derived cell engraftment levels on the cystine content and *Ctns* expression in the kidney of the treated *Ctns*<sup>-/-</sup> mice, we measured cystine content by mass spectrometry and *Ctns* gene expression by reverse transcription-qPCR comparing treated mice and controls. Cystine content was significantly decreased in the kidneys of treated *Ctns*<sup>-/-</sup> mice compared with *Ctns*<sup>-/-</sup> control mice (54% decrease, Table 2). However, linear regression analyses showed that kidney cystine levels are independent of the donor-derived cell engraftment levels ( $F_{1,28} = 3.384$ ,  $P = 0.076$ ). Moreover, renal function data did not depend on the cystine levels in the kidney ( $F_{1,27} = 0.833$ ,  $P = 0.370$  for creatinine, and  $F_{1,27} = 2.191$ ,  $P = 0.150$  for urea). Cystine levels of treated *Ctns*<sup>-/-</sup> mice were significantly reduced in comparison with *Ctns*<sup>-/-</sup> controls in all the other tissues tested; the decrease ranged from 56.5% in the muscle to 96.5% in the liver (Table 2).

As expected, no *Ctns* expression was detected in *Ctns*<sup>-/-</sup> control mice. In parallel, *Ctns* expression measured by reverse transcription-qPCR was observed in kidneys from treated mice (12,225 ± 12,823-fold change) and wild-type mice (316,209 ± 251,247-fold change). Linear regression analysis showed that *Ctns* expression within the kidney significantly increased with increasing blood engraftment levels ( $F_{1,27} = 6.394$ ,  $P = 0.018$ ,  $R^2 = 0.437$ ). Similarly, an analysis of variance of *Ctns* expression in the kidney using the dichotomous variable of greater or less than 50% donor-derived

engraftment levels demonstrated the same positive correlation (11,982 ± 5052 versus 6765 ± 6690;  $P = 0.01$ ).

#### Histology confirms the biochemical data

The histology of non-treated *Ctns*<sup>-/-</sup> mice at 15–17 months of age consistently exhibited severe kidney anomalies characterized by their multifocal distribution covering a mean 81% (range 50–95%) of the cortex. The lesions primarily affected proximal tubules and were characterized by atrophy to complete disappearance of epithelial cells and thickening of the tubular basement membranes (Figure 2a and c). Corresponding medullary tubules were collapsed and obstructed by protein casts. Within atrophic areas, glomerular tufts can appear collapsed or sclerotic. Large and multiple mononuclear infiltrates were present at the corticomedullary junctions. In contrast, interstitial fibrosis was not a major finding in the mouse model of cystinosis, which correlates to that seen in the human.<sup>18</sup> Treated *Ctns*<sup>-/-</sup> mice exhibited similar anomalies but, in most of the mice with high blood engraftment, their extent was less extensive than in the non-treated mice (Figure 2b). Moreover, fewer and smaller lymphoid infiltrates were observed in the treated mice (Figure 2b and d) than in the *Ctns*<sup>-/-</sup> control mice (Figure 2a and c).

We scored the kidney histology from wild-type controls, *Ctns*<sup>-/-</sup> and treated mice, with scores ranging from 1 to 6 based on the % extent of cortical damage (see Materials and Methods). The average score for wild-type mice was 1.1 ± 0.3; some of the transplanted wild-type mice exhibiting renal anomalies, such as focal tubular dilatation, presence of a few medullary casts, or focal glomerulosclerosis, possibly as a consequence of irradiation and aging (data not shown). The average score for *Ctns*<sup>-/-</sup> mice was 5.1 ± 0.9 versus 4.6 ± 1.4 for treated mice. Furthermore, even if the difference was not significant, the score of treated mice with a donor-derived cell engraftment level >50% was lower compared with treated mice with blood engraftment levels <50% (4.1 ± 1.6 versus 5.4 ± 0.7), confirming the renal function data obtained from biochemical measurements.

Kidney sections stained with methylene blue in ethanol were used to observe cystine crystals. Low magnification pictures of kidney sections were taken and analyzed using ImageJ software (see Materials and Methods). Abundant

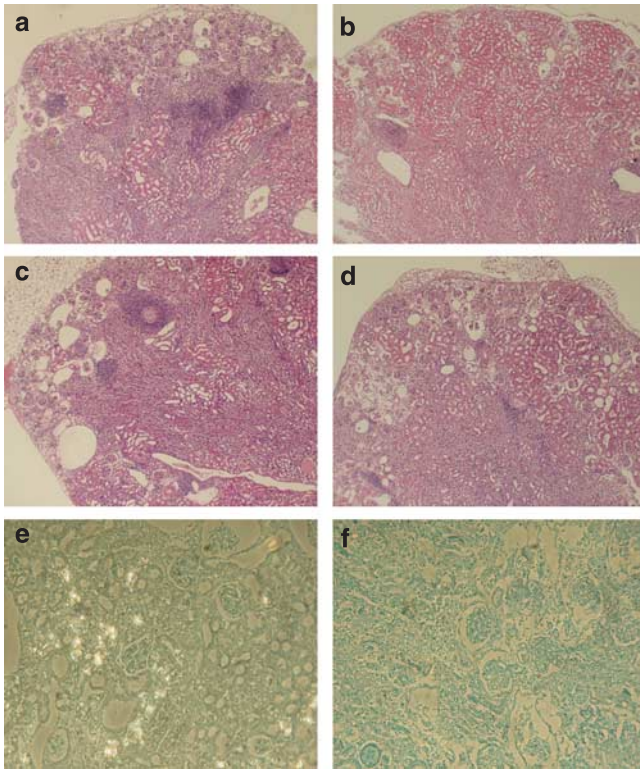


**Figure 2 | Histological analyses of kidney sections. Kidney anomalies observed in treated and non-treated *Ctns*<sup>-/-</sup> mice.**

Histological pictures of kidney sections stained with hematoxylin and eosin (a-d) and methylene blue (e, f). (a, c) *Ctns*<sup>-/-</sup> mice controls exhibit severe kidney anomalies characterized by their multifocal distribution. Proximal tubules were atrophic or completely disappeared, and less frequently tubules were dilated. Glomerular tufts were normal, collapsed, or sclerotic. Large and multiple mononuclear infiltrates were present at the corticomedullary junction. (b) Treated *Ctns*<sup>-/-</sup> mice with high blood engraftment exhibited the same histological anomalies but to a much lesser extent than in the non-treated mice. (d) Fewer lymphoid infiltrates were observed in the treated mice even with important histological anomalies. (e) Abundant cystine crystals are observed in non-treated *Ctns*<sup>-/-</sup> mice. (f) Very few cystine crystals are observed in treated *Ctns*<sup>-/-</sup> mice even with a damaged kidney.

cystine crystals were observed in kidney sections from non-treated *Ctns*<sup>-/-</sup> mice whereas none or few crystals were detected in kidney sections from treated mice (683 pixels  $\pm$  567 versus 57 pixels  $\pm$  63 respectively,  $P < 0.000001$ ; Figure 2e and f). Even treated mice with low donor-derived cell engraftment, and thus very damaged kidneys, exhibited no or few cystine crystals (Figure 2f).

### Characterization of the BM-derived renal interstitial cells

We previously showed that most of the transplanted bone marrow-derived cells were interstitial in the kidney of treated *Ctns*<sup>-/-</sup> mice and few co-localized with proximal tubular cells.<sup>19</sup> In this long-term analysis, we did not observe any bone marrow-derived epithelial cells but rather abundant interstitial GFP<sup>+</sup> cells in the kidney of treated mice. In the healthy area of the kidneys, bone marrow-derived cells

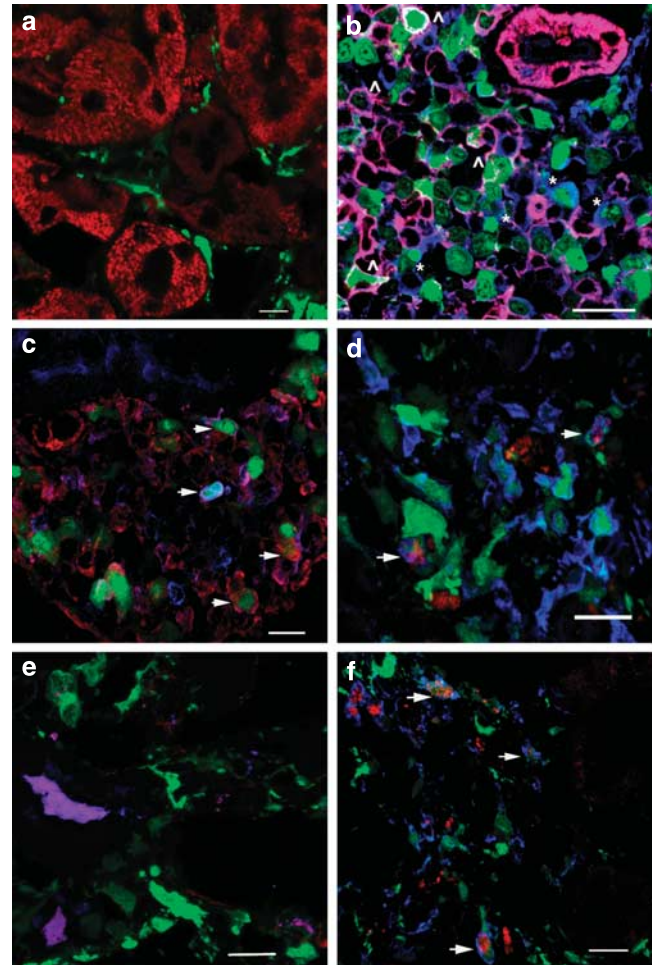


**Figure 3 | Characterization of bone marrow-derived green fluorescent protein (GFP)<sup>+</sup> cells within the kidney of 15-17-month-old *Ctns*<sup>-/-</sup> mice.**

Representative Z-series confocal microscopy pictures of treated *Ctns*<sup>-/-</sup> mice's kidney sections. Transplanted, bone marrow-derived GFP<sup>+</sup> cells are seen in green. (a) Proximal tubular staining by Lotus Tetragonolobus lectin (red). GFP<sup>+</sup> cells are interstitial and appear elongated around the tubes. (b) Renal cortical fibroblasts expressing CD73 are seen in blue and MHC class II expressing interstitial cells are seen in red. Some GFP<sup>+</sup> cells express either CD73 (\*) or MHC class II-labeled cells (Λ). (c) Some GFP<sup>+</sup> cells express both  $\alpha$  smooth muscle actin (red) and CD73 (blue) and thus are myofibroblasts (arrows). (d) Some GFP<sup>+</sup> cells are dendritic cells (arrows) stained with both MHC class II (blue) and CD11c (red). (e) No colocalization was observed between GFP<sup>+</sup> cells and conventional dendritic cells stained by both CD11c (red) and CD103 (blue). (f) Some GFP<sup>+</sup> cells belong to the inflammatory dendritic cell subset (arrows) stained with both CD11c (red) and F4/80 (blue). Bars = 10  $\mu$ m (a, b), 15  $\mu$ m (c, e), and 20  $\mu$ m (d, f).

appeared elongated and beneath the tubular basement membrane (Figure 3a). In the areas of focal cortical injury, we observed that many GFP<sup>+</sup> cells were fibroblasts-like cells expressing ecto-5'-nucleotidase (CD73), and others expressing both CD73 and  $\alpha$ -smooth muscle actin were myofibroblasts (Figure 3b and c). Some cortical GFP<sup>+</sup> interstitial cells were dendritic cells stained by both MHC class II and CD11c (Figure 3d). However, they were mostly part of the

inflammatory dendritic cell subset (CD11c<sup>+</sup> and F4/80<sup>+</sup>; Figure 3f), as opposed to conventional dendritic cells (CD11c<sup>+</sup> and CD103<sup>+</sup>; Figure 3e). Finally, we noticed that bone marrow-derived GFP<sup>+</sup> cells expressing CD45, a pan-leukocyte marker, were present in juxtamedullary infiltrates as well as in atrophic scars (data not shown). In the kidney of transplanted wild-type mice, very few GFP<sup>+</sup> cells were observed even after a year post transplantation (data not shown), which confirmed our previous findings that bone marrow-derived cell integration within the kidney occurred specifically in injured kidney.<sup>19</sup>

## DISCUSSION

We previously showed that transplantation of BMCs and HSCs expressing a functional *Ctns* gene led to a significant cystine decrease in all tissues as well as the preservation of kidney function at 4 months post transplantation in the mouse model for cystinosis.<sup>19</sup> The present study represents the long-term follow-up of treated mice, age of 15–17 months. Three important conclusions can now be drawn from this new work: (1) transplantation of bone marrow stem cells expressing a functional *Ctns* gene significantly decreases long-term cystine accumulation in all tested tissues including kidneys (from 56.5% decrease in the muscle to 96.5% in the liver), (2) transplantation of bone marrow stem cells expressing a functional *Ctns* gene can provide long-term protection to the kidney, and (3) there is a threshold for the level of donor-derived blood cell engraftment necessary for preservation of kidney histology and function, and this correlates with increased expression of the *Ctns* gene in the kidney.

These results suggesting correlations between therapeutic success in the kidney and levels of transplanted cell engraftment may provide new insights into the controversial field of using adult bone marrow stem cells for kidney repair. We propose that differences in the levels of engraftment may explain some of the discrepancies and non-reproducibility of previously reported results. Some authors showed that BMCs could migrate to damaged kidneys and reverse renal dysfunction.<sup>7–11</sup> By contrast, other studies showed that BMCs could not generate renal cells or impact kidney injury.<sup>12–16</sup> In our mouse model of cystinosis, the data presented demonstrate that, in the context of chronic and progressive renal damage, bone marrow-derived cells can efficiently engraft in the kidney, generate interstitial renal cells, and decrease progression of kidney dysfunction if the level of *Ctns*-expressing cells engrafted in the bone marrow is sufficient. These data could also explain the lack of improvement of acute tubular damage by transplanted BMCs in non-irradiated mice.<sup>23</sup> Even if transplanted cells were engrafted in the bone marrow, the level of donor cell engrafted was probably too low (~30%).

Moreover, the kinetics and/or the mechanism of cell death in the kidney might be important to generate the necessary stimuli driving stem cell mobilization, migration, and integration in the kidney. We showed previously and

confirmed here that, in contrast to the treated *Ctns*<sup>-/-</sup> mice, few bone marrow-derived cells are engrafted in the kidneys of wild-type mice transplanted with the syngeneic GFP<sup>+</sup> cells. These results support the conclusion that renal injury is a necessary factor. However, the extent and chronicity of the cystinosis injury is also important. This hypothesis is supported by studies in a mouse model of Hepatorenal Tyrosinemia, Type 1 (HT1). HT1 is characterized by the accumulation of fumarylacetoacetate due to the lack of fumarylacetoacetate hydrolase (*FAH*) expressed in liver and proximal tubular cells.<sup>24</sup> Affected patients develop both liver injury and renal Fanconi syndrome.<sup>25</sup> The mouse model is neonatal lethal, but animals can survive if treated with cyclohexanedione.<sup>26</sup> However, renal tubule repopulation by *Fah*<sup>+</sup> bone marrow stem cells did not occur presumably because of the mild renal disease in these treated mice.<sup>27</sup> Similarly, no renal tubule repopulation was observed after induction of acute tubular necrosis. Therefore, the investigators modified the HT1 model to induce chronic renal injury by backcrossing the *Fah*<sup>-/-</sup> mice to the homogentisic acid dioxygenase-deficient mice, an enzyme upstream of *Fah* in the pathway, leading to the accumulation of the toxic fumarylacetoacetate substrate in the proximal tubules. As a consequence, there was a dramatic increase in the repopulation of renal tubules (up to 50%) and correction of the kidney dysfunction. Thus, we propose that another reason for discrepancies in different models might be differences in the extent and chronicity of the renal injury particularly as many of the studied models represent dramatic acute injury.

Surprisingly, we did not observe any correlation between renal function and cystine content, indicating that kidney damage is not directly linked to cystine levels in this compartment. This is further supported by the fact that none or few cystine crystals were observed in kidney sections from treated *Ctns*<sup>-/-</sup> mice, even in the animals with low blood engraftment levels and extensive kidney damage. Thus, these new results show that bone marrow-derived cells specifically lead to the correction of the cells containing cystine crystals, which are probably apoptotic.<sup>28,29</sup> They also demonstrate that the accumulation of tissue cystine in the kidney is not the only cause of the tissue injury in cystinosis. This is relevant to the pathophysiology of the cystinosis nephropathy in human patients, which remains incompletely understood.<sup>29–33</sup> Thus, proximal tubulopathy is typically found as early as 6 months of age whereas the multi-compartment tissue injuries correlated with increased onset of cystine crystals occur after 10 years of age.<sup>34</sup>

Bone marrow-derived cells are localized mostly in the interstitium within the kidneys of *Ctns*<sup>-/-</sup> mice transplanted with BMCs or HSCs expressing a functional *Ctns* gene. These cells differentiated into lymphoid, dendritic, or fibroblastic/myofibroblastic cells. We showed by confocal microscopy that the majority of the bone marrow-derived (for example, GFP<sup>+</sup>) dendritic cells are inflammatory type dendritic cells that we propose are involved in kidney repair by inhibiting the inflammatory response, as suggested by others.<sup>35</sup> In this

context, we showed that fewer and smaller mononuclear cell infiltrates were consistently observed in the treated mice than in the *Ctns*<sup>-/-</sup> mice controls. Moreover, as we are not demonstrating that the bone marrow-derived cells are simply replacing the kidney epithelium, the obvious question is how do these interstitial cells protect the cystinotic kidneys. BMCs could indirectly affect tubule regeneration or preservation as suggested previously.<sup>13</sup> One possibility could be the intercellular transfer of the cystinosis protein or mRNA from the bone marrow-derived interstitial cells to the epithelium. A second possibility is that these interstitial cells provide some kind of survival factors protecting the nearby epithelial cells from injury. In the context of acutely injured kidney, Fujigaki *et al.*<sup>36</sup> showed that fibroblastic cells develop increased number of cytoplasm-containing microfilament bundles extending into the tubular basement membranes and in parallel differentiate into myofibroblasts.

Finally, we showed that there is no significant difference in the preservation of renal function between mice transplanted before and after 6 months of age, suggesting that if the renal anomalies are not too advanced, BMC transplantation in older animals can still contribute to the preservation of the kidney. This is important for cystinotic patients as they now live longer with oral cysteamine therapy and eventually develop chronic kidney disease. Thus, we propose that bone marrow transplantation, even in young adults, could still allow the survival of their kidneys. However, our results suggest that there is a necessary engraftment threshold such that the quantity of cells expressing *Ctns* gene in the bone marrow will determine the success of this therapy. We also showed that HSC transplantation modeled in mice by purification of Sca1<sup>+</sup> HSCs has the same therapeutic effects as whole BMC transplantation in the mouse model of cystinosis. This has a significant implication for the clinical translation of these data to patients, as human HSCs (CD34<sup>+</sup>) have the advantages to be easily isolated from the peripheral blood after growth factor-mediated mobilization (that is, granulocyte macrophage colony-stimulating factor). All these data will have to be carefully considered in the design of any future clinical trial using adult bone marrow stem cells for cystinosis and possibly for other hereditary nephropathies.

## MATERIALS AND METHODS

### Mice

C57BL/6 *Ctns*<sup>-/-</sup> mice were provided by Dr C. Antignac (Inserm U983, Paris, France) and bred continuously at The Scripps Research Institute. Transgenic mice constitutively expressing GFP (C57BL/6-Tg(ACTB-EGFP)10sb/J) were obtained from The Jackson Laboratory, Bar Harbor, MI. All protocols were approved by the AAALAC (Accredited Institutional Animal Care and Use Committee of The Scripps Research Institute).

### BMC and HSC isolation and cell transplantation

BMCs were flushed from the long bones of 6–8-week-old GFP mice and transplanted without further culture or processing.

Sca1<sup>+</sup> HSCs were sorted using anti-Sca1 antibody conjugated to mini-magnetic beads (Miltenyi Biotec, Auburn, CA). Cells were injected via the tail vein in 2–10-month-old mice. All mice were lethally irradiated (cesium radiation, 8 Gy) on the day preceding the injection. To analyze engraftment, fresh blood was treated with red blood cell lysis buffer (eBioscience, San Diego, CA) and subsequently analyzed by flow cytometry to quantify GFP<sup>+</sup> cells. Lineage-specific staining and flow cytometry allowed determination of the hematopoietic chimerism for T cells (Cy-chrome-conjugated anti-CD3ε; BD Biosciences Pharmingen, San Jose, CA), B cells (phycoerythrin-conjugated anti-CD19; BioLegend, San Diego, CA), and macrophages (phycoerythrin-conjugated MAC3; BD Biosciences Pharmingen). Appropriate isotype controls were used for each. Mice were killed between 15 and 17 months of age.

### Blood and urine analysis

Serum was obtained by cardiac puncture, and 24 h urine samples were collected in metabolic cages before killing the mice. Serum and urine phosphate levels as well as serum creatinine, urea, and alkaline phosphatase were estimated by using colorimetric assays according to the manufacturer's recommendations (BioAssay Systems, Hayward, CA). Protein levels in urine were measured using Pierce BCA Protein Assay Kit (Rockford, IL).

### Cystine content measurement

Explanted tissues were grounded in 500 μl of *N*-ethylmaleimide (Fluka Biochemika, Bushs, Switzerland) at 650 μg/ml for cystine measurements. The proteins were precipitated using 15% 5-sulfosalicylic acid dihydrate (Fluka Biochemika), resuspended in 0.1 N NaOH and measured using the Pierce BCA protein assay kit. The cystine-containing supernatants were sent to the UCSD Biochemical Genetics laboratory (San Diego, CA) for measurements by stable isotope dilution high performance liquid chromatography-electrospray ionization tandem mass spectrometry using a Teicoplanin (CHIROBIOTIC T, Sigma, St Louis, MO) column and specific transitions (MRM).

### Quantitative reverse transcription-PCR

RNA was isolated from explanted kidneys by homogenization in 750 μl Trizol LS Reagent (Invitrogen). Phase separation was performed with the addition of 200 μl chloroform followed by centrifugation. After removal of the aqueous phase, RNA was recovered by precipitating with isopropyl alcohol. RNA was purified using the RNeasy mini-protocol for RNA cleanup, including column DNase treatment (Qiagen, Valencia, CA). A total of 1 μg of RNA for each tissue was reverse transcribed using iScript cDNA Synthesis Kit (Bio-Rad, Hercules, CA). *Ctns*-specific qPCR was performed using 2 μl of cDNA and 2× Universal TAQ man master mix (Roche Diagnostics, Indianapolis, IN), *Ctns* primer mix (in *Ctns* exon 8: *Ctns* oligo 1: 5'-TTGTGGCTGCAGTCGGTATC-3', *Ctns* oligo 2: 5'-AGCTTGATGTAGGAGAAGCA GAAGA-3', and *Ctns* probe: 5'-CACATGGCTCCAGTTC-3'

(Applied Biosystems, Foster City, CA)), and 18S primer mix (Applied Biosystems) on an Applied Biosystems 7900 HT. The expression level of *Ctns* gene, expressed as fold change, was calculated using the  $\Delta\Delta C_t$  method between the target gene and an endogenous control (18S).

### Histology

Kidneys were fixed in formalin and embedded in paraffin. Sections were stained with hematoxylin and eosin or briefly stained with methylene blue in absolute alcohol for the detection of cystine crystals. Slides were reviewed in a blinded fashion by one of us (Dr MC Gubler). In cystinotic mice, kidney lesions develop focally in the cortex and between focal scars the renal parenchyma is preserved. Blinded scoring was done from 1 to 6 based on the extent of cortical damage estimated in % terms: 1 (0–10% damaged kidney), 2 (10–30%), 3 (30–50%), 4 (50–70%), 5 (70–90%), and 6 (>90%). Cystine crystals were quantified using ImageJ software on low magnification pictures of methylene blue-stained sections covering most of the kidney section for each mouse. The threshold was adjusted to recognize specifically the cystine crystals, and pixels were quantified.

### Immunofluorescence analysis

Kidneys were fixed in 5% formaldehyde for 30 min, equilibrated in 20% sucrose overnight and frozen in Tissue-Tek Optimal Cutting Temperature buffer at  $-80^{\circ}\text{C}$  (Sakura Finetek USA, Torrance, CA). Sections of 12  $\mu\text{m}$  were blocked with 1% bovine serum albumin, 10% donkey or goat serum in phosphate buffer saline. The blocking buffer was then diluted 1:5 in phosphate buffer saline and used to dilute the antibodies as denoted below, all secondary antibodies were diluted 1:100 and incubated with the sections for 1 h at room temperature. We used the directly labeled Alexa 647-conjugated anti-F4/80 (1:25 dilution) and Alexa Fluor 647 phalloidin (1:500 dilution, Molecular Probes, Eugene, OR). We also used the biotinylated-conjugated Lotus Tetragonolobus lectin (1:100 dilution, Vector Laboratories, Burlingame, CA), anti-mouse CD45 (1:200 dilution), and anti-mouse I-A/I-E MHC class II (1:200 dilution, BD Pharmingen), followed by streptavidin Alexa 594 (Molecular Probes). Kidney sections were also stained with the rat anti-mouse CD73 (1:200 dilution) and CD103 (1:100 dilution; BD Pharmingen), followed by goat anti-rat conjugated with Cy5 (Jackson ImmunoResearch, West Grove, PA). Finally, we used the monoclonal anti- $\alpha$ -smooth muscle actin (clone 1A4, 1:200 dilution; Sigma) followed by goat anti-mouse conjugated with Texas Red (Jackson ImmunoResearch), and the hamster anti-mouse CD11c antibody (1:50 dilution, BD Pharmingen) followed by goat anti-hamster conjugated with DyLight 594 (Jackson ImmunoResearch). All slides were counterstained with 4,6-diamidino-2-phenylindole (1:500 dilution in phosphate buffer saline for 30 min, Molecular Probes). Images were acquired using a Zeiss LSM 710 laser scanning confocal microscope attached to a Zeiss Observer Z1 inverted microscope (BioRad-Carl Zeiss, Thornwood, NY). All images were 8-bit optical image

slices (0.5  $\mu\text{m}$  interval step slices) acquired using Zen 2009 software (Carl Zeiss MicroImaging GmbH, Thornwood, NY). Images were then analyzed with IMARIS 6.5 imaging software (Bitplane Scientific Solutions, Saint Paul, MN) to generate 3-D reconstruction series of optical slices (Z-stacks).

### Statistics

We summarized continuous data as arithmetic means  $\pm$  s.d. Group comparisons of renal function parameters were made with parametric analyses of variance, followed by Tukey's HSD (Honestly Significant Difference) procedure for pairwise comparisons. Associations between blood engraftment and renal function were investigated with linear regressions. All analyses were performed in Systat 12 (Systat Software, Chicago, IL, 2007).  $P < 0.05$  was considered as statistically significant. Differences in histology scores across the different groups were compared with the Kruskal–Wallis test, followed by Dunn's multiple comparison procedure.

### DISCLOSURE

All the authors declared no competing interests.

### ACKNOWLEDGMENTS

We gratefully acknowledge Dr Corinne Antignac for providing the *Ctns*<sup>-/-</sup> mice and for her expert assistance in the correction of the manuscript. This work was funded by the Cystinosis Research Foundation.

### REFERENCES

1. Consortium CKDP. Association of estimated glomerular filtration rate and albuminuria with all-cause and cardiovascular mortality in general population cohorts: a collaborative meta-analysis. *Lancet* 2010; **375**: 2073–2081.
2. Black C, Sharma P, Scotland G *et al*. Early referral strategies for management of people with markers of renal disease: a systematic review of the evidence of clinical effectiveness, cost-effectiveness and economic analysis. *Health Technol Assess* 2010; **14**: 1–184.
3. Cerasola G, Nardi E, Palermo A *et al*. Epidemiology and pathophysiology of left ventricular abnormalities in chronic kidney disease: a review. *J Nephrol* 2010; **24**: 1–10.
4. Cantley LG. Adult stem cells in the repair of the injured renal tubule. *Nat Clin Pract Nephrol* 2005; **1**: 22–32.
5. De Broe ME. Tubular regeneration and the role of bone marrow cells: 'stem cell therapy'—a panacea? *Nephrol Dial Transplant* 2005; **20**: 2318–2320.
6. Masereeuw R. Contribution of bone marrow-derived cells in renal repair after acute kidney injury. *Minerva Urol Nefrol* 2009; **61**: 373–384.
7. Fang TC, Alison MR, Cook HT *et al*. Proliferation of bone marrow-derived cells contributes to regeneration after folic acid-induced acute tubular injury. *J Am Soc Nephrol* 2005; **16**: 1723–1732.
8. Fang TC, Otto WR, Rao J *et al*. Haematopoietic lineage-committed bone marrow cells, but not cloned cultured mesenchymal stem cells, contribute to regeneration of renal tubular epithelium after HgCl<sub>2</sub> 2 - induced acute tubular injury. *Cell Prolif* 2008; **41**: 575–591.
9. Li B, Cohen A, Hudson TE *et al*. Mobilized human hematopoietic stem/progenitor cells promote kidney repair after ischemia/reperfusion injury. *Circulation* 2010; **121**: 2211–2220.
10. LeBleu V, Sugimoto H, Mundel TM *et al*. Stem cell therapies benefit Alport syndrome. *J Am Soc Nephrol* 2009; **20**: 2359–2370.
11. Sugimoto H, Mundel TM, Sund M *et al*. Bone-marrow-derived stem cells repair basement membrane collagen defects and reverse genetic kidney disease. *Proc Natl Acad Sci USA* 2006; **103**: 7321–7326.
12. Lin F, Moran A, Igarashi P. Intrarenal cells, not bone marrow-derived cells, are the major source for regeneration in postischemic kidney. *J Clin Invest* 2005; **115**: 1756–1764.
13. Duffield JS, Park KM, Hsiao LL *et al*. Restoration of tubular epithelial cells during repair of the postischemic kidney occurs independently of bone marrow-derived stem cells. *J Clin Invest* 2005; **115**: 1743–1755.

14. Szczypka MS, Westover AJ, Clouthier SG *et al.* Rare incorporation of bone marrow-derived cells into kidney after folic acid-induced injury. *Stem Cells* 2005; **23**: 44–54.
15. Stokman G, Leemans JC, Claessen N *et al.* Hematopoietic stem cell mobilization therapy accelerates recovery of renal function independent of stem cell contribution. *J Am Soc Nephrol* 2005; **16**: 1684–1692.
16. Stokman G, Leemans JC, Stroo I *et al.* Enhanced mobilization of bone marrow cells does not ameliorate renal fibrosis. *Nephrol Dial Transplant* 2008; **23**: 483–491.
17. Cherqui S, Sevin C, Hamard G *et al.* Intralysosomal cystine accumulation in mice lacking cystinosis, the protein defective in cystinosis. *Mol Cell Biol* 2002; **22**: 7622–7632.
18. Nevo N, Chol M, Bailleux A *et al.* Renal phenotype of the cystinosis mouse model is dependent upon genetic background. *Nephrol Dial Transplant* 2009; **25**: 1059–1066.
19. Syres K, Harrison F, Tadlock M *et al.* Successful treatment of the murine model of cystinosis using bone marrow cell transplantation. *Blood* 2009; **114**: 2542–2552.
20. Baer PC, Geiger H. Mesenchymal stem cell interactions with growth factors on kidney repair. *Curr Opin Nephrol Hypertens* 2010; **19**: 1–6.
21. Kunter U, Rong S, Djuric Z *et al.* Transplanted mesenchymal stem cells accelerate glomerular healing in experimental glomerulonephritis. *J Am Soc Nephrol* 2006; **17**: 2202–2212.
22. Tögel F, Cohen A, Zhang P *et al.* Autologous and allogeneic marrow stromal cells are safe and effective for the treatment of acute kidney injury. *Stem Cells Dev* 2009; **18**: 475–485.
23. Fang TC, Otto WR, Jeffery R *et al.* Exogenous bone marrow cells do not rescue non-irradiated mice from acute renal tubular damage caused by HgCl<sub>2</sub>, despite establishment of chimaerism and cell proliferation in bone marrow and spleen. *Cell Proliferat* 2008; **41**: 592–606.
24. St-Louis M, Tanguay RM. Mutations in the fumarylacetoacetate hydrolase gene causing hereditary tyrosinemia type I: overview. *Hum Mutat* 1997; **9**: 291–299.
25. Grompe M. The pathophysiology and treatment of hereditary tyrosinemia type 1. *Semin Liver Dis* 2001; **21**: 563–571.
26. Grompe M, Lindstedt S, al-Dhalimy M *et al.* Pharmacological correction of neonatal lethal hepatic dysfunction in a murine model of hereditary tyrosinaemia type I. *Nat Genet* 1995; **10**: 453–460.
27. Held PK, Al-Dhalimy M, Willenbring H *et al.* *In vivo* genetic selection of renal proximal tubules. *Mol Ther* 2006; **13**: 49–58.
28. Thoene JG. Lysosomal cystine augments apoptosis and causes the phenotype in cystinosis. *Beijing Da Xue Xue Bao* 2005; **37**: 8–9.
29. Thoene JG. A review of the role of enhanced apoptosis in the pathophysiology of cystinosis. *Mol Genet Metab* 2007; **92**: 292–298.
30. Chol M, Nevo N, Cherqui S *et al.* Glutathione precursors replenish decreased glutathione pool in cystinotic cell lines. *Biochem Biophys Res Commun* 2004; **324**: 231–235.
31. Coor C, Salmon RF, Quigley R *et al.* Role of adenosine triphosphate (ATP) and NaK ATPase in the inhibition of proximal tubule transport with intracellular cystine loading. *J Clin Invest* 1991; **87**: 955–961.
32. Foreman JW, Benson LL, Wellons M *et al.* Metabolic studies of rat renal tubule cells loaded with cystine: the cystine dimethylester model of cystinosis. *J Am Soc Nephrol* 1995; **6**: 269–272.
33. Sakarcan A. The Fanconi syndrome of cystinosis: insights into the pathophysiology. *Turk J Pediatr* 2002; **44**: 279–282.
34. Gahl WA, Thoene J, Schneider JA. Cystinosis: a disorder of lysosomal membrane transport. In: Scriver CR, Beaudet AL, Sly WS, Valle D (eds). *The Metabolic and Molecular Bases of Inherited Disease*, 8th edn, vol. 3. McGraw Hill: New York, 2001, pp 5085–5108.
35. Kim MG, Boo CS, Ko YS *et al.* Depletion of kidney CD11c+ F4/80+ cells impairs the recovery process in ischaemia/reperfusion-induced acute kidney injury. *Nephrol Dial Transplant* 2010; **25**: 2908–2921.
36. Fujigaki Y, Muranaka Y, Sun D *et al.* Transient myofibroblast differentiation of interstitial fibroblastic cells relevant to tubular dilatation in uranyl acetate-induced acute renal failure in rats. *Virchows Arch* 2005; **446**: 164–176.